Life Sciences 239 (2019) 117040

Contents lists available at ScienceDirect

Life Sciences

journal homepage: www.elsevier.com/locate/lifescie

TBX3 deficiency accelerates apoptosis in cardiomyoblasts through regulation of P21 expression

Meiling Cao[a], Binlu Zhu[b], Yuanyuan Sun[c], Xueqi Zhao[b], Guangrong Qiu[c], Weineng Fu[c], Hongkun Jiang[b,*]

[a] Department of Neonatology, The First Affiliated Hospital of China Medical University, Shenyang, 110001, People's Republic of China
[b] Department of Pediatrics, The First Affiliated Hospital of China Medical University, Shenyang, 110001, People's Republic of China
[c] Department of Medical Genetics, College of Basic Medical Sciences, China Medical University, Shenyang, 110122, People's Republic of China

ARTICLE INFO

Keywords:
Congenital heart disease
TBX3
Cell cycle arrest
Apoptosis

ABSTRACT

Congenital heart disease (CHD) is the most common birth defect in newborns. There is increasing evidence that apoptosis and remodeling of the cardiomyoblasts are the major pathology of CHD. Previous research found that T-box transcription factor 3 (TBX3) was compulsory for the regulation of proliferation, cell cycle arrest and apoptosis in various cells. Hence, TBX3 might be involved in the treatment of CHD. The primary aim of this study was to study the effects of TBX3 on apoptosis in aged cardiomyoblasts and investigate the latent mechanism. In the present study, we found TBX3 knockdown induced proliferation inhibition, cell cycle arrest and apoptosis accompanied by mitochondrial dysfunction in cardiomyoblasts at passage 10 to 15. Apoptosis-inducing effects of TBX3 silence could be neutralized by silencing P21 using specific siRNA. In addition, the mRNA and protein expression levels of TBX3 in the heart tissues of sporadic type CHD donors were obviously down-regulated. In conclusion, we demonstrated that TBX3 deficiency accelerated apoptosis via directly regulating P21 expression in senescent cardiomyoblasts.

1. Introduction

Congenital heart disease (CHD), the leading non-infectious cause of morbidity and mortality in newborn children in the world, is a life-threatening congenital malformation associated with genetic backgrounds and environmental risk factors. According to the clinical manifestation, CHD can be classified into two types, including acyanotic congenital heart disease and cyanotic congenital heart disease [1,2]. An increasing number of epidemiological investigations found that the incidence of CHD was 19–75 of every 1000 living newborns [3]. If the infants who did not survive were calculated, CHD incidence would be higher [4,5]. Despite simple CHD can be completely remitted at present, early surgical management that has high risk is the necessary therapeutic strategy for complex CHD. As known, although multi-gene abnormalities have been confirmed in the occurrence of CHD, the accurate mechanism of CHD is remained to be investigated. Programmed cell death plays a crucial part in maintaining normal cardiac function under physiological conditions and apoptosis-related protein is expressed at the basal level in the postnatal hearts [6,7]. A clinical assessment indicated that aggravated apoptosis could be found in the cardiac tissue samples from CHD patients compared with the normal heart tissues from the aged-matched subjects [8]. In addition, promoting proliferation and suppressing apoptosis exerted protective effects in H9C2 cardiomyoblasts, highlighting that apoptosis inhibition might be a potential therapeutic strategy for CHD [9,10]. Hence, we believe that inhibition of apoptosis in cardiomyoblasts might be a promising therapeutic strategy to inhibit CHD development.

T-box transcription factor 3 (TBX3) belongs to the T-box factor family that is composed of evolutionary conserved transcription factors regulating early embryonic development [11]. TBX3 has established role in the development of the heart, mammary glands, limbs and genitalia in the vertebrates [12]. In addition, human TBX3 gene mutation leads to ulnar-mammary syndrome (UMS), which is characterized by upper limb malformation, mammary hypoplasia, as well as deficiency in hair, tooth and reproductive system [13,14]. On the contrary, the oncogenic effects of TBX3 overexpression have emerged in

Abbreviations: ATPase, adenosine triphosphatase; CDK, cyclin dependent kinase; CHD, congenital heart disease; ROS, reactive oxygen species; TBX3, T-box transcription factor 3; UMS, ulnar-mammary syndrome

* Corresponding author. Department of Pediatrics, The First Affiliated Hospital of China Medical University, 155 North Nanjing Street, Shenyang, 110001, People's Republic of China.
E-mail address: jianghongkun1217@126.com (H. Jiang).

https://doi.org/10.1016/j.lfs.2019.117040
Received 22 July 2019; Received in revised form 23 October 2019; Accepted 31 October 2019
Available online 06 November 2019
0024-3205/

a wide variety of cancer, including gastric cancer, breast cancer and pancreatic cancer [15–17]. A recent study showed that the occurrence and development of conotruncal heart defect could be attributed to the variants of TBX3 [18]. Hence, the effects of TBX3 in cardiomyoblasts are worth to be emphasized in CHD. Except for the definite regulation role on the development of multiple organs, TBX3 expression possesses the function on modulating cell cycle. The previous experiments have shown that the protein expression of TBX3 is elevated at S phase and TBX3 silence results in S phase arrest, indicating the regulation of TBX3 in cell cycle [19]. Moreover, the previous study also has illustrated that the function of TBX3 on overriding cell cycle to inhibit apoptosis and enhance proliferation is achieved by suppressing cell cycle regulatory protein P21 (also named as P21 waf1/cip1 and P21/CDKN1A) [19]. As the downstream signaling molecule of P53, P21 serves as the inhibitor of CDK family in both P53-dependent and P53-independent manners, which is necessary for adjusting cell cycle and proliferation [20]. Cell cycle transitions (G1 phase to S phase and G2 phase to mitosis) is depended on continuous activation and inactivation of CDK proteins that are attached to serine/threonine protein kinases [21]. For instance, the activation of CDK4 and CDK6 by cyclin D1 senses the mitogenic signals and serves as the growth factor sensors in G1 phase, cyclin E1 and E2-induced CDK activation triggers the transition from G1 phase to S phase [22]. Plus, the first identified CKI protein P21 suppresses diverse cell cycle progression through disrupting the interactions between CDKs and cyclin proteins [23]. Several lines of evidence demonstrate that the mitochondrion involves in regulation of apoptosis in mammals. Mitochondria are the cellular bioenergy centers in a physiological manner [24]. In addition to participating in regulation of energy generation, intercellular communication and metabolism, the importance of mitochondria in apoptosis has been well established [25]. Cytochrome C migrates from mitochondrial inter-membrane space to the cytoplasm and triggers the apoptosis-related events at molecular levels [26]. Cytosolic cytochrome C interacts with Apaf-1, recruits procaspase-9, assembles cytochrome *c*/Apaf-1/caspase-9 apoptosomes, and thereby initiating downstream apoptotic cascade [27]. These events above suggested that TBX3 might be the important bond between the pathogenesis of CHD and pathological apoptosis as well as cell cycle arrest in cardiomyoblasts. Therefore, the effects of TBX3 in the pathogenesis of CHD are worthy to be investigated.

Here we aimed to investigate the effects of TBX3 on mitochondrial function, apoptosis and cell cycle arrest in aged H9C2 cardiomyoblasts and explore the potential mechanism of CHD occurrence.

2. Materials and methods

2.1. Cell treatment

2.1.1. Cell culture

Rat cardiomyoblast H9C2 cell line was obtained from Zhong Qiao Xin Zhou Biotechnology Co., Ltd. (Shanghai, China). H9C2 cardiomyoblasts at passage 10 to 15 were employed. H9C2 cardiomyoblasts were grown in Dulbecco's modifed Eagle's medium (DMEM) (Gibco, USA) supplemented with 10% fetal bovine serum (FBS) (Hyclone, USA) at 37 °C with 5% CO_2 in a humidified incubator.

2.1.2. Transfection

H9C2 cardiomyoblasts at passage 10 to 15 were transfected with TBX3-specific small interfering RNA (siRNA) 1–5 or control siRNA (Wanlei Biological Technology Co., Ltd., Shenyang, China) according to the instructions. Then, the transfected H9C2 cardiomyoblasts were maintained in fresh culture medium for 48 h before the transfection efficiency detection.

The sequences for TBX3 siRNA1-5 and control siRNA were listed as follows:

TBX3 siRNA-1: 5′-CCAUGAGAGAUCCGGUUAUTT-3’
5′-AUAACCGGAUCUCUCAUGGTT-3’
TBX3 siRNA-2: 5′-GCGAAUGUUCCCUCCAUUUTT-3’
5′-AAAUGGAGGGAACAUUCGCTT-3’
TBX3 siRNA-3: 5′-GCUGAUGACUGUCGAUAUATT-3’
5′-UAUAUCGACAGUCAUCAGCTT-3’
TBX3 siRNA-4: 5′-CCAACAACAUUUCGGAUAATT-3’
5′-UUAUCCGAAAUGUUGUUGGTT-3’
TBX3 siRNA-5: 5′-GCAGUCCAUGAGGGUGUUUTT-3’
5′-AAACACCCUCAUGGACUGCTT-3’
Control siRNA: 5′-UUCUCCGAACGUGUCACGUTT-3’
5′-ACGUGACACGUUCGGAGAATT-3’

2.1.3. Transduction

H9C2 cardiomyoblasts at passage 10 to 15 were transduced with TBX3-expressing lentivirus or negative control lentivirus (Wanlei Biological Technology Co., Ltd., Shenyang, China) and all the transduction protocols were carried out according to the manufacturer's instruction. Afterwards, the transduced H9C2 cardiomyoblasts were maintained in fresh culture medium for 48 h before harvest.

2.2. Real-time polymerase chain reaction (RT-PCR)

After the corresponding treatment, the total RNA of aforementioned H9C2 cardiomyoblasts or heart samples was extracted by using Trizol reagent. After TBX3 cDNA was synthesized by using the M-MLV reverse transcriptase (TianGEN, China), RT-PCR analysis was conducted with SYBR Green master mix kits in the Exicycler 96 System (Bioneer, Korea). TBX3 mRNA level was normalized to that of GAPDH and calculated by $2^{-\triangle\triangle CT}$ method.

The primers for RT-PCR were as follows:

Rat TBX3 forward: 5′-TCGGATAAACACGGATTTACTT-3’; reverse: 5′-GTTGGCTCTGACGATGTGG-3’

Rat GAPDH forward: 5′-ACGTTGACATCCGTAAAGAC-3’; reverse: 5′-TAGGAGCCAGGGCAGTAA-3’

Human TBX3 forward: 5′-GGCATCCCGTTCTCCTCCCT-3’; reverse: 5′-TCGCCTTCCCGACTTGGT-3’

Human GAPDH forward: 5′-GACCTGACCTGCCGTCTAG-3’; reverse: 5′-AGGAGTGGGTGTCGCTGT-3’

2.3. Cell counting kit-8 (CCK-8) assay

To assess the viability of aged H9C2 cardiomyoblasts following treatment, H9C2 cardiomyoblasts at passage 10 to 15 were seeded in plates at a density of 5×10^3 cells/well. After the transfection or transduction described above, the H9C2 cardiomyoblasts were incubated for another 0, 24 or 48 h before the exposure to CCK8 solution (KeyGEN BioTECH, China) according to the manufacturer's instructions. The absorbance at 450 nm was measured by a microplate reader.

2.4. Cell cycle analysis

Cell cycle distribution of the aforementioned H9C2 cardiomyoblasts was analyzed by using flow cytometry. To be brief, H9C2 cardiomyoblasts at passage 10 to 15 were harvested 48 h after the respective treatment, fixed in 70% ethanol at 4 °C for 2 h, treated with propidium iodide (PI) dye (Beyotime Institute of Biotechnology, China) at 37 °C for 30 min, and subsequently analyzed by using a flow cytometer (NovoCyte, United States).

2.5. Hochest 33342 staining

Hoechst 33342 staining was implemented to observe the apoptotic morphological characteristics of aged H9C2 cardiomyoblasts. Simply, H9C2 cardiomyoblasts at passage 10 to 15 were plated in a 6-well plate at a density of 1×10^5 cells/well. Following the transfection or transduction protocol, the H9C2 cardiomyoblasts were incubated for another 48 h, washed with PBS, and stained by Hoechst 33342 according to the

manufacturer's instruction. Finally, apoptotic morphological alterations in the stained H9C2 cardiomyoblasts were observed under a fluorescence microscope at 400 × magnification.

2.6. Apoptosis analysis

The influence of TBX3 expression on apoptosis in aged H9C2 cardiomyoblast was examined using flow cytometry. Simply, H9C2 cardiomyoblasts at passage 10 to 15 were plated in a 6-well plate at a density of 1×10^5 cells/well. Following the transfection or transduction protocol, the H9C2 cardiomyoblasts were stained by adding Annexin V-fluorescein isothiocyanate (FITC) and PI in dark at room temperature for 10–20 min finally, apoptosis rate of the treated H9C2 cardiomyoblasts was detected by using a flow cytometer (NovoCyte, United States).

2.7. Mitochondrial membrane potential detection

The changes of mitochondrial membrane potential in aforementioned H9C2 cardiomyoblasts were detected by using specific fluorescent probe JC-1 according to the requirement of mitochondrial membrane potential detection kit (Beyotime Institute of Biotechnology, China). The relative fluorescence intensity (excitation and emission wavelengths of 485 and 525 nm, excitation and emission wavelengths of 525 and 590 nm, respectively) represented the change of mitochondrial membrane potential.

2.8. Adenosine triphosphatase (ATPase) activity

Treated H9C2 cardiomyoblasts were lysed with PBS and the protein concentrations of lysis were determined by BCA protein quantification kit (Beyotime Institute of Biotechnology, China). In short, the activity of ATPase in H9C2 cardiomyoblasts was quantified by corresponding commercial kits (Nanjing Jiancheng Bioengineering Institute, China). The activity of ATPase was expressed as U per milligram protein (U/mg prot).

2.9. Mitochondrial reactive oxygen species (ROS) production

Mitochondria of the H9C2 cardiomyoblasts at passage 10 to 15 were separated by centrifugation as recommended by the manufacturer (Beyotime Institute of Biotechnology, China). The separated mitochondria were incubated with 10 μM fluorescence probe DCFH-DA for 30 min at 37 °C followed by fluorescence intensity detection according to the instructions of ROS detection kit (Beyotime Institute of Biotechnology, China).

2.10. Immunofluorescence

H9C2 cardiomyoblasts at passage 10 to 15 were treated as described in cell treatment, fixed with 4% paraformaldehyde for 15 min, and then incubated with 0.1% tritonX-100 (Beyotime Institute of Biotechnology, China) for 30 min at room temperature. After wash with PBS for three times, the treated H9C2 cardiomyoblasts were incubated with primary Ki67 antibody (Cell Signaling Technology, United States, dilution: 1:100) overnight at 4 °C followed by Cy3-labeled goat anti-rabbit IgG (H + L) (Solarbio, China). Afterwards, 4', 6-diamidino-2-phenylindole (DAPI, Beyotime Institute of Biotechnology, China) incubation was utilized to stain the nuclei. Finally, immune-positive H9C2 cardiomyoblasts were observed under a fluorescence microscope at 400 × magnification.

2.11. Chromatin immunoprecipitation (ChIP) assay

ChIP assay was implemented to detect the targeted relationship between TBX3 and P21. Briefly, the aforementioned H9C2 cardiomyoblasts were fixed in 1% formaldehyde solution at room temperature for 10 min, washed with PBS, and harvested by centrifugation at 2000 rpm for 5 min. The chromatin was isolated and exposed to sonication to obtain DNA fragments (fractionated size: 500–1000 bp) that were in turn immunoprecipitated with TBX3 antibody. Afterwards, the TBX3 protein-bound DNA was purified by a DNA purifcation kit (Wanlei Biological Technology Co., Ltd., Shenyang, China). Finally, the purified DNA was utilized to analyze the combination between TBX3 and P21.

2.12. Western blot

The mitochondrial and total protein samples were isolated from the aforementioned H9C2 cardiomyoblasts. Briefly, the same amount of protein samples were separated by 8%, 10% or 14% sodium dodecyl sulfate polyacrylamide gel electrophoresis (SDS-PAGE) and transferred onto PVDF membranes (Millipore, USA) that were subsequently blocked by 5% non-fat milk for 1 h at the room temperature. Afterwards, the PVDF membranes were subjected to the relevant primary antibody at 4 °C overnight, respective horseradish peroxidase (HRP) labeled secondary antibody (Solarbio, China) for 45 min at 37 °C, and ultimately the ECL kit (Solarbio, China). The quantification of the protein expression was implemented by Gel-Pro-Analyzer software.

The primary antibodies were as follows: TBX3 (Abcam, UK), cyclin A (Abcam, UK), cyclin D1 (Cell Signaling Technology, United States), cyclin B1 (Cell Signaling Technology, United States), caspase-3 (Boster, China), cleaved caspase-3 (Cell Signaling Technology, United States), caspase-9 (Abcam, UK), cleaved caspase-9 (Cell Signaling Technology, United States), Bcl-2 (proteintech, China), Bax (proteintech, China), cleaved-PARP (Cell Signaling Technology, United States), cytochrome C (Cell Signaling Technology, United States), P21 (Abclonal, China).

2.13. Patient samples

Eight heart samples from CHD fetuses (24–25 weeks) were recruited in the First Affiliated Hospital of China Medical University. The sporadic types of CHD included ventricular septal defect, atrioventricular septal defect and atrial septal defect. Eight healthy hearts came from fetuses (24–25 weeks) with other congenital defects. Heart tissue collection was implemented after abortion. RT-PCR and TBX3 ELISA (USCN, China) were used to detect heart TBX3 mRNA and protein levels. The procedures were in accordance with the Declaration of Helsinki and the protocols were accordance with the Ethics Committee of the First Affiliated Hospital of China Medical University.

2.14. Statistical analysis

Data were presented as mean ± standard derivations (SD) and calculated by GraphPad Prism 7.0 (GraphPad Software, United States). Significant differences between two groups were analyzed by *t*-test and data from three or more groups was determined using one way analysis of variance (ANOVA) followed by a Tukey's multiple comparison test. Value of p less than 0.05 was considered statistically significant. All in vitro experiments were performed three times (n = 3).

3. Results

3.1. Effect of TBX3 on proliferation in H9C2 cardiomyoblasts

CCK-8 assay was utilized to inspect the influence of TBX3 expression on proliferation of H9C2 cardiomyoblasts. We used TBX3 specific siRNA to silence CXCR2 gene in H9C2 cardiomyoblasts, meanwhile, TBX3-expressing lentivirus was used to induce TBX3 overexpression (**Supplement** Figs. S1–2). As shown in Fig. 1A, TBX3 knockdown significantly decreased H9C2 cardiomyoblast viability in a time dependent manner. On the contrary, H9C2 cardiomyoblast proliferation could be

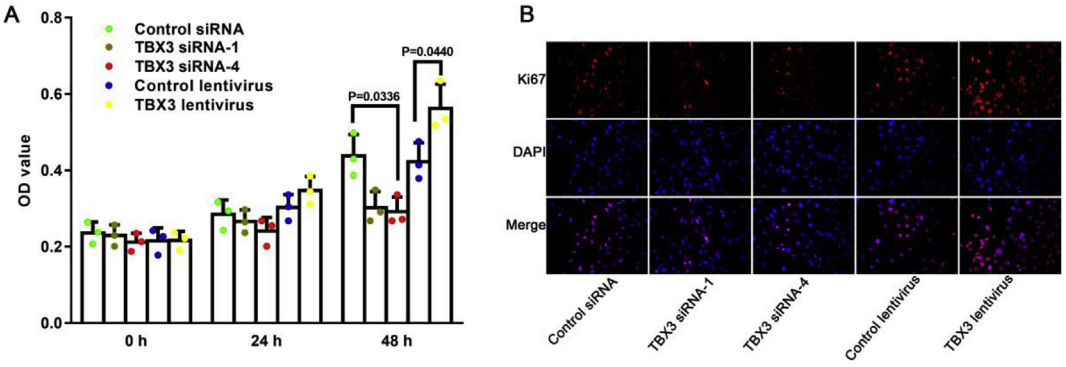

Fig. 1. Effect of TBX3 on proliferation in H9C2 cardiomyoblasts. (A) CCK-8 was used to evaluate the effect of TBX3 expression on viability in H9C2 cardiomyoblasts. (B) Immunofluorescence targeting Ki67 in treated H9C2 cardiomyoblasts. Data were represented as mean ± SD at least three independent experiments. The data from three or more groups were analyzed by one-way analysis of variance (ANOVA) followed by Tukey's multiple comparison test.

elevated with TBX3 overexpression. Similar to the results of CCK8, the fluorescence targeting the proliferation markers Ki67 was whittled with TBX3 silence while enhanced with TBX3 overexpression in H9C2 cardiomyoblasts (Fig. 1B). The above results indicated that TBX3 silence accelerated proliferation deficiency in H9C2 cardiomyoblasts.

3.2. Effect of TBX3 on cell cycle arrest in H9C2 cardiomyoblasts

To investigate whether TBX3 expression was involved in cell cycle arrest, we analyzed the distribution of H9C2 cardiomyoblast cell cycle following TBX3 expression interference. As exhibited in Fig. 2A, compared with the control group, there was a significant increase in the percentage of H9C2 cardiomyoblasts at G1 phase ($p < 0.05$) while an obvious decrease at S phase ($p < 0.05$) after TBX3 specific siRNA treatment. However, TBX3 overexpression did not markedly affected cell cycle distribution in H9C2 cardiomyoblasts. In addition, TBX3 silence inhibited the expression of cyclin protein family, including cyclin D1, cyclin A and cyclin B1 (Fig. 2B–D, $p < 0.05$). Interestingly, TBX3 overexpression could aggrandize cyclin protein expression while did not regulate cell cycle in H9C2 cardiomyoblasts. The data indicated that TBX3 knockdown accelerated cell cycle arrest at S phase in H9C2 cardiomyoblasts.

3.3. Effect of TBX3 on apoptosis in H9C2 cardiomyoblasts

Since apoptosis is a consequence of cell cycle arrest, we employed Hoechst 33342 staining to observe apoptosis morphology and Annexin V FITC/PI double staining to quantify cell apoptosis rate in H9C2 cardiomyoblasts after TBX3 expression interference. As shown in Fig. 3A, TBX3 siRNA-treated H9C2 cardiomyoblasts exhibited typical morphological characteristics of apoptosis, including nuclear fragmentation and chromatin condensation. Afterwards, the percentage of apoptotic H9C2 cardiomyoblasts was assessed by Annexin V FITC/PI double staining and the data showed that TBX3 silence dramatically induced apoptosis in H9C2 cardiomyoblasts (Fig. 3B–C, $p < 0.05$). Subsequently, western blot was also conducted to investigate the levels of Apoptosis related proteins, such as cleaved caspase-9, cleaved caspase-3, cleaved PARP, Bcl-2 and Bax. The results demonstrated an increase in the levels of cleaved caspase-9, cleaved caspase-3, cleaved PARP and Bax, and a decrease in Bcl-2 after TBX3 knockdown in H9C2 cardiomyoblasts (Fig. 3D–H, $p < 0.05$). However, there was no significant change in apoptotic state of TBX3-overexpressing H9C2 cardiomyoblasts. The results indicated that TBX3 knockdown was involved in H9C2 cardiomyoblast apoptosis.

3.4. Effect of TBX3 on mitochondrial function in H9C2 cardiomyoblasts

To further examine the effects of TBX3 expression on mitochondrial function in H9C2 cardiomyoblasts, we first detected the alterations of mitochondrial membrane potential by utilizing the JC-1 fluorescent dye. As shown in Fig. 4A, the ratio between the red and green fluorescence in H9C2 cardiomyoblasts loaded with JC-1 staining was significantly down-regulated after TBX3 knockdown ($p < 0.05$). Then mitochondrial ATPase activity and ROS generation were also analyzed. The results showed that mitochondrial ATPase activity was down-regulated (Fig. 4B, $p < 0.05$) and ROS generation was up-regulated (Fig. 4C, $p < 0.05$) in H9C2 cardiomyoblasts with TBX3 knockdown, which indicated the existence of mitochondrial dysfunction. Besides, as exhibited in Fig. 4D–E, the cytochrome C content in the cytoplasm was prominently increased while decreased in the mitochondria after TBX3 siRNA treatment, indicating TBX3 knockdown accelerated cytochrome C release from the mitochondria into the cytoplasm in H9C2 cardiomyoblasts. The results indicated that TBX3 knockdown induced mitochondrial disorder in in H9C2 cardiomyoblasts.

3.5. Effect of TBX3 on p21 expression in H9C2 cardiomyoblasts

To investigate the underlying mechanism of TBX3 expression on cell cycle and apoptosis, we detected cell cycle regulatory protein P21 levels in H9C2 cardiomyoblasts after TBX3 expression interference. As shown in Fig. 5A–B, both the mRNA and protein levels of P21 were increased in H9C2 cardiomyoblasts with TBX3 knockdown ($p < 0.05$). Moreover, the interaction between TBX3 protein and P21 DNA was verified by ChIP assay (Fig. 5C). The results indicated that P21 gene expression was directly regulated by TBX3 protein.

3.6. Effect of TBX3/p21 pathway on proliferation in H9C2 cardiomyoblasts

To verify the effect of TBX3/p21 pathway on proliferation in H9C2 cardiomyoblasts, TBX3 siRNA and p21 siRNA were co-transfected into H9C2 cardiomyoblasts. As shown in Fig. 6A, P21 expression was obviously suppressed after the co-transfection compared with TBX3 siRNA transfection alone ($p < 0.05$). Additionally, the decreased proliferation capacity induced by TBX3 silence could be observably promoted by TBX3 siRNA and p21 siRNA co-transfection in H9C2 cardiomyoblasts (Fig. 6B), manifesting that TBX3/p21 pathway might participate in the regulation of proliferation in H9C2 cardiomyoblasts.

3.7. TBX3 expression in CHD samples

Finally, we examined the mRNA and protein expression of TBX3 in the hearts of CHD donors to verify its potential in CHD treatment. As shown in Fig. 7A and B, the mRNA and protein expression levels of TBX3 were obviously decreased in donors with sporadic type CHD compared with the control ones ($p < 0.05$), indicating the importance of TBX3 in CHD treatment.

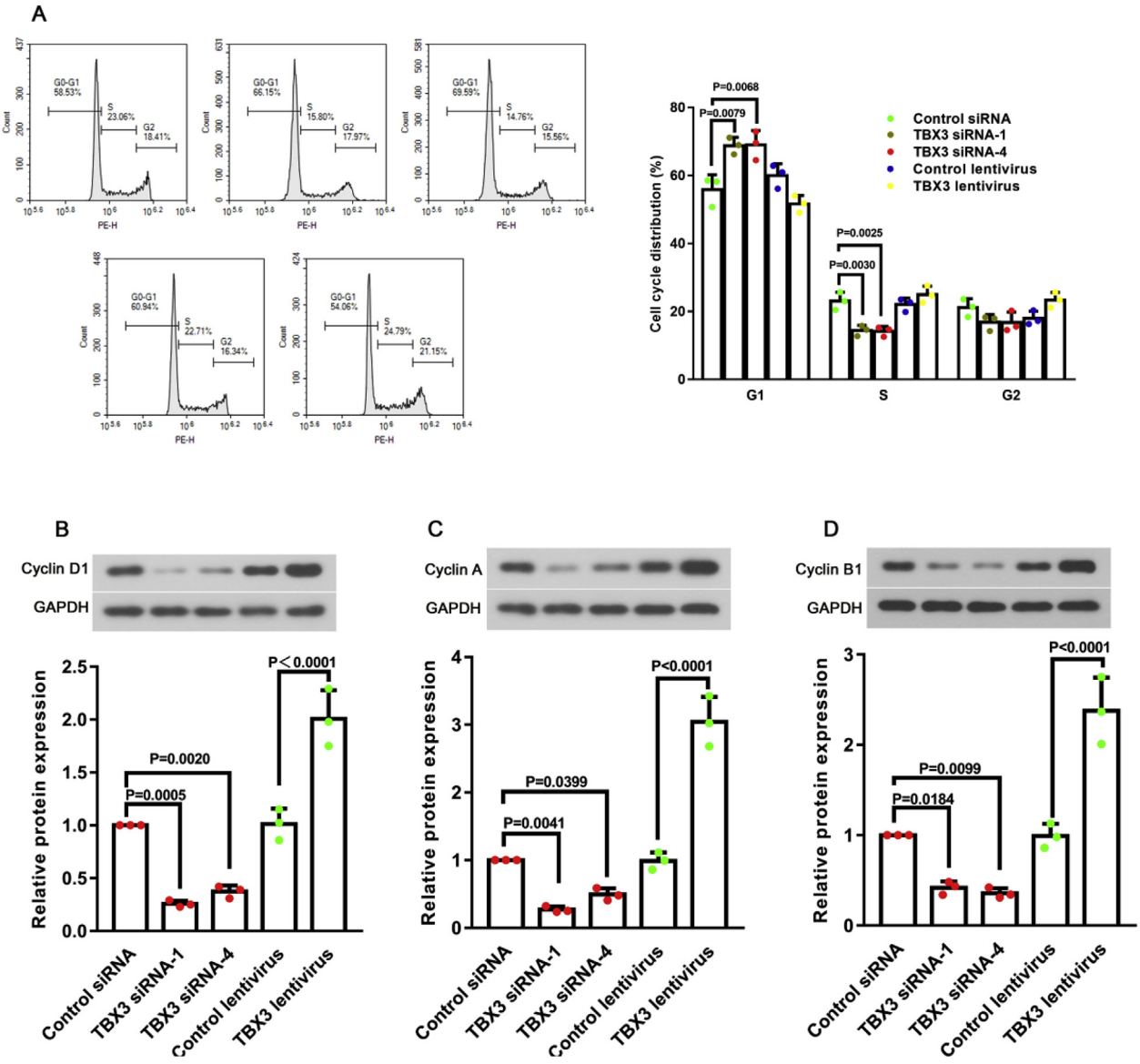

Fig. 2. Effect of TBX3 on cell cycle arrest in H9C2 cardiomyoblasts. (A) Flow cytometry was used to analyze cell cycle distribution in H9C2 cardiomyoblasts. Representative western blot for (B) Cyclin D1, (C) Cyclin A and (D) Cyclin B1 in H9C2 cardiomyoblasts. Data were represented as mean ± SD at least three independent experiments. The data from three or more groups were analyzed by one-way analysis of variance (ANOVA) followed by Tukey's multiple comparison test.

4. Discussion

Pathological cardiomyoblast loss is a major histopathological hallmark of CHD, but the accurate molecular mechanisms still need future investigation. In the present study, we investigated whether TBX3 expression deficiency was the key point of accelerating mitochondrial dysfunction, cell cycle arrest and apoptosis in aged H9C2 cardiomyoblasts. We found that TBX3 silence by specific siRNA inhibited proliferation and blocked G1/S phase transition in aged H9C2 cardiomyoblasts. TBX3 knockdown up-regulated aged H9C2 cardiomyoblast apoptosis accompanied by mitochondrial dysfunction. Besides, the apoptosis induction of TBX3 deletion in aged H9C2 cardiomyoblasts could be abolished by P21 knockdown. Interestingly, exorbitant proliferate was not observed in H9C2 cardiomyoblast with TBX3 overexpression. Hence, our results manifested that TBX3 was an important mediator that regulated proliferation and apoptosis by targeting P21 in aged H9C2 cardiomyoblasts.

TBX3 is a critical member of the highly conserved T-box family of transcription factors that possess explicit regulatory role on development in vertebrates [28]. Moreover, TBX3 involves in cell fate decision, cell cycle regulation, organ development and even oncogenesis [29]. In addition, a strong relationship between TBX3 insufficiency and congenital developmental disorders has been reported in the literature [30]. As mentioned in the aforementioned literature, TBX3 variants could be observed in patients with conotruncal heart defects, a heterogeneous congenital heart malformation [18]. In our study, we found TBX3 deficiency in the hearts of donors with sporadic types of CHD, which indicated its clinical importance in CHD treatment. Afterwards, in order to further verify the effects of TBX3 expression on the cell proliferative potential in aged H9C2 cardiomyoblasts, we employed TBX3 specific siRNA to silence TBX3 and TBX3-expressing lentivirus to increase TBX3 in H9C2 cells at passage 10 to 15. After the corresponding treatment, the mRNA and protein levels of TBX3 were respectively up-regulated and down-regulated in H9C2 cardiomyoblasts (**Supplement** Figs. S1–2). Besides, the inhibiting effects of TBX3 silence did not appear until 48 h after TBX3 specific siRNA employment.

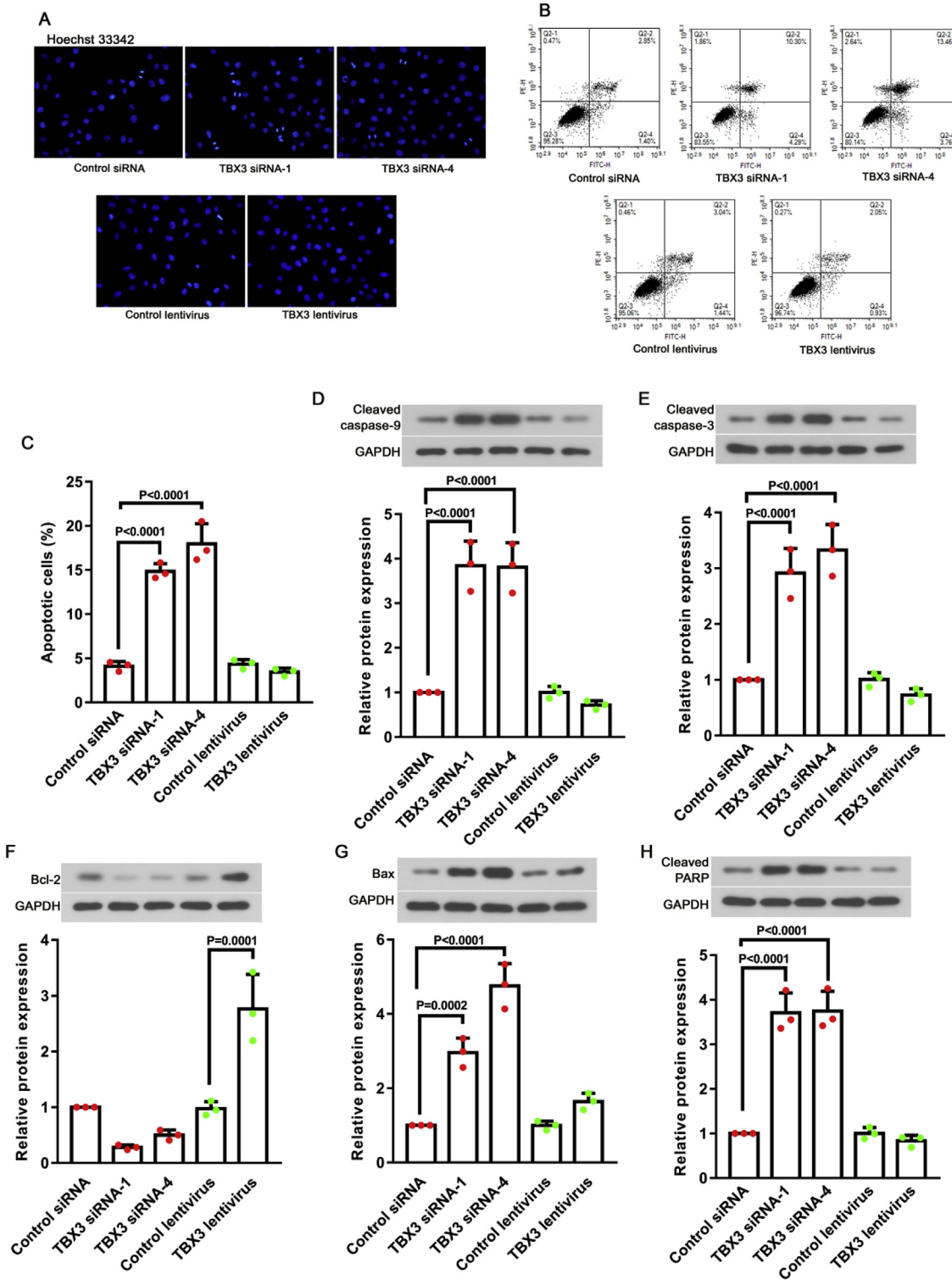

Fig. 3. Effect of TBX3 on apoptosis in H9C2 cardiomyoblasts. (A) Representative images of Hoechst 33342 staining at 400 × magnification in H9C2 cardiomyoblasts. (B) Annexin V FITC/PI double staining and (C) apoptosis rate of H9C2 cardiomyoblasts were detected by using a flow cytometer. Representative western blot for (D) cleaved caspase-9, (E) cleaved caspase-3 and (F) Bcl-2, (G) Bax and (H) cleaved PARP in H9C2 cardiomyoblasts. Data were represented as mean ± SD at least three independent experiments. The data from three or more groups were analyzed by one-way analysis of variance (ANOVA) followed by Tukey's multiple comparison test.

Similarly, the effects of promoting growth were detected 48 h after TBX3-expressing lentivirus transduction. It is well understood that Ki67 protein expressed at all stages of the cell cycle other than resting phase is an approved cellular marker labeling proliferative potential in several cell types [31]. Hence, we utilized immunofluorescence targeting Ki67 to verify cellular proliferation in aged H9C2 cardiomyoblasts 48 h after treatment and the results were in line with CCK8 analysis. Based on these data, we confirmed that the abnormal expression of TBX3 was involved in the regulation of proliferation in aged H9C2 cardiomyoblasts.

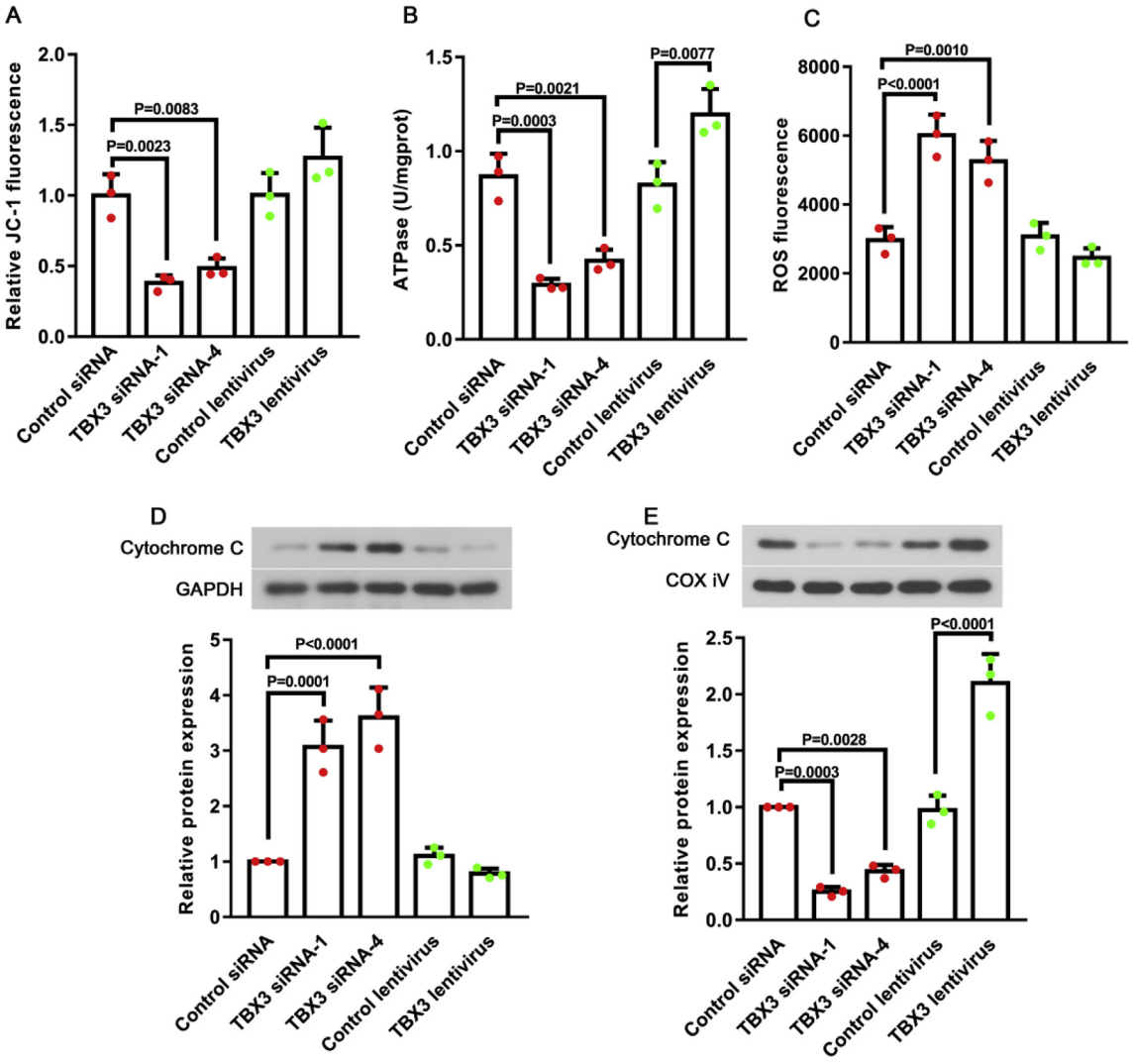

Fig. 4. Effect of TBX3 on mitochondrial function in H9C2 cardiomyoblasts. (A) The alteration of mitochondrial membrane potential in H9C2 cardiomyoblasts. (B) The activity of ATPase in H9C2 cardiomyoblasts. (C) Fluorescence intensity of ROS in H9C2 cardiomyoblasts. Representative western blot for (D) cytochrome C in the cytoplasm and (E) cytochrome C in the mitochondria of H9C2 cardiomyoblasts. The data from three or more groups were analyzed by one-way analysis of variance (ANOVA) followed by Tukey's multiple comparison test.

It is well accepted that transition from G1 phase to S phase and G2 phase to M phase are the two critical stage of the cell cycle. In addition, cell growth can be inhibited, if the cell cycle is blocked at any phase. Prior studies that have suggested the importance of TBX3 expression on inducing cell cycle arrest through blocking G1/S transition [19]. Subsequently, the effects of TBX3 expression on the distribution of cell cycle in H9C2 cardiomyoblasts were investigated by using flow cytometry. We also observed that the percentage of aged H9C2 cardiomyoblast at G1 phase was increased while decreased in S phase, indicating the diminished DNA synthesis after TBX3 knockdown. Since cell cycle was triggered by CDKs and their regulatory subunit cyclins, we found cyclin D1, cyclin A and cyclin B1 levels were decreased in TBX3 siRNA-treated H9C2 cardiomyoblasts. Wondrously, TBX3 knockdown inhibited cell proliferation and triggered cell cycle arrest, but TBX3 over-expression is ineffective for the cell cycle in aged H9C2 cardiomyoblasts, the mechanism of which needed further investigation.

Since cell cycle arrest is an induction factor of apoptosis, which is considered to participate in pathological changes of diverse cardiac disorders, such as myocarditis and cardiomyopathy [7]. Although apoptosis is occurred at base levels under the physiological circumstance, excessive cardiomyoblast apoptosis can be detected in CHD patients with volume overload [32]. Recently, inhibiting apoptosis and elevating survival of cardiomyoblasts have been proposed as the promising treatment strategies targeting CHD. Based on the above, we tried to evaluate changes in apoptosis morphology, apoptosis index and apoptosis-related protein expression in modified H9C2 cardiomyoblasts. The data of current study demonstrated that apoptosis was promoted after TBX3 silence in aged H9C2 cardiomyoblasts. Moreover, mitochondrial dysfunction characterized by decreased mitochondrial membrane potential, suppressed ATPase activity and elevated ROS generation was also detected in TBX3-silenced H9C2 cardiomyoblasts. Since apoptosis could be affected by multifarious intracellular transduction cascades, we only explored the pathway associated with cell cycle arrest. As an inhibitor of CDKs, P21 is known to possess multiple biological functions, such as regulating cell cycle, differentiation and apoptosis [33]. Nonetheless, the effect of P21 on apoptosis is bidirectional. This is mainly because P21 expression induces cell cycle blockage to repair DNA damage when the cell suffers mild DNA lesions, whereas P21 triggers apoptotic response once the DNA damage exceeds the repair ability [34]. In order to investigate the role of P21 in modified H9C2 cardiomyoblasts, we co-transfected TBX3 siRNA and P21 siRNA into aged H9C2 cardiomyoblasts. In our study, P21 silence abolished the apoptosis-inducing effects of TBX3 deficiency. Combined the CHIP assay, we found P21 was the direct downstream signaling

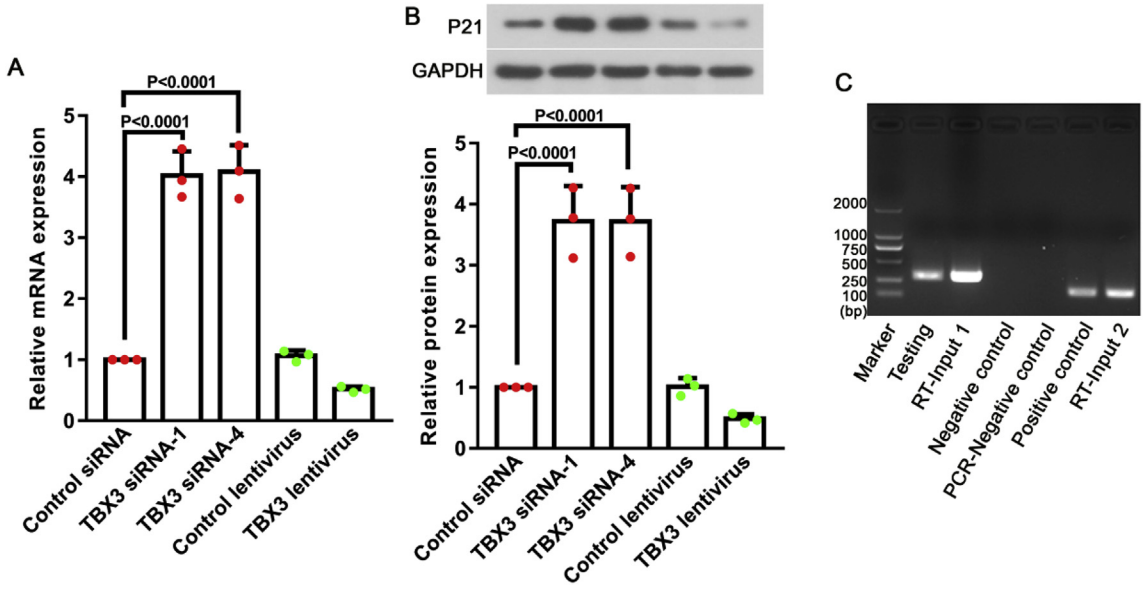

Fig. 5. Effect of TBX3 on p21 expression in H9C2 cardiomyoblasts. The relative (A) mRNA and (B) protein levels of P21 in H9C2 cardiomyoblasts. (C) ChIP was used to verify the targeted combination between TBX3 and p21 in H9C2 cardiomyoblasts. Negative control: control IgG; Positive control: anti-RNA Polymerase II; PCR-negative control: distilled H_2O; RT-Input 1: P21; RT-Input 2: GAPDH. The data from three or more groups were analyzed by one-way analysis of variance (ANOVA) followed by Tukey's multiple comparison test.

molecule of TBX3. Based on the data above, we summarized TBX3/P21 signaling was involved in apoptotic occurrence in aged H9C2 cardiomyoblasts.

H9C2 cardiomyoblasts at passage 10 to 15 were employed in the present study. Prior studies have suggested that morphology changes and sensitivity to toxicity are increased with the number of passages in H9C2 cardiomyoblasts [35]. However, the literature results also indicated that the influence of cell line passage number on the reliability of study results was intricate and depended on multi-factor, such as culture conditions [35]. Hence, we will investigate the effect of TBX3 deficiency on apoptosis in cardiomyoblasts at different passage in the future.

In conclusion, the present study showed that TBX3 expression deficiency accelerated apoptosis in aged cardiomyoblasts, which was accompanied by mitochondrial dysfunction, cell cycle arrest, growth suppression and apoptosis. Although more research should be

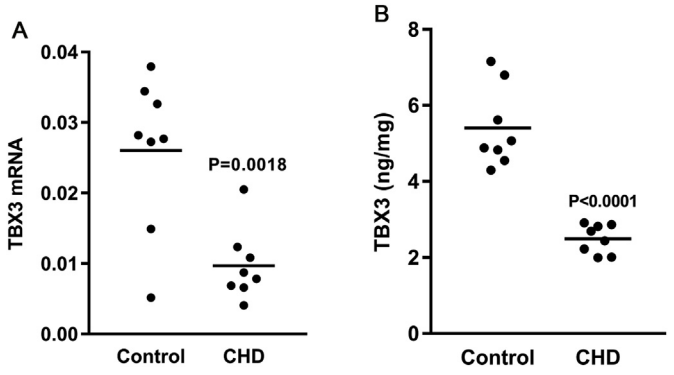

Fig. 7. TBX3 expression in CHD samples. TBX3 mRNA (A) and protein (B) levels in the heart tissues of CHD donors. The data from two groups was determined by *t*-test.

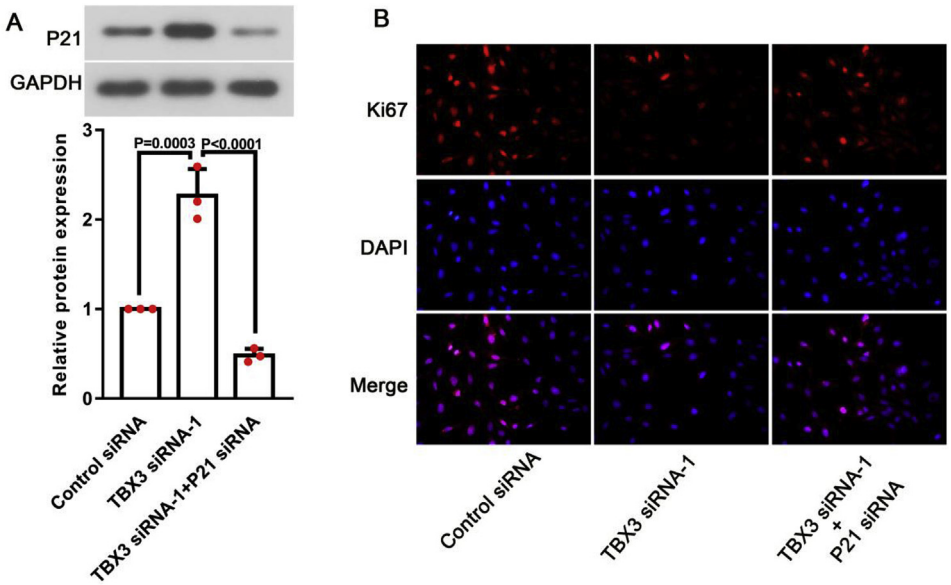

Fig. 6. Effect of TBX3/p21 pathway on proliferation in H9C2 cardiomyoblasts. (A) The relative protein levels of P21 in H9C2 cardiomyoblasts. (B) Immunofluorescence targeting Ki67 in H9C2 cardiomyoblasts. The data from three or more groups were analyzed by one-way analysis of variance (ANOVA) followed by Tukey's multiple comparison test.

implemented to verify the accurate mechanism of TBX3 expression on cardiomyoblast function, our work suggests TBX3 maybe one of the potential therapeutic targets of CHD.

Declaration of competing interest

The authors declared no conflict of interest.

Acknowledgement

This study was supported by grants from the National Natural Science Foundation of China (No. 81300130) and the Basic Scientific Research Projects of Liaoning Higher Education Institutions (No. LFWK201701).

Appendix A. Supplementary data

Supplementary data to this article can be found online at https://doi.org/10.1016/j.lfs.2019.117040.

References

[1] T. Van Der Bom, A.C. Zomer, A.H. Zwinderman, F.J. Meijboom, B.J. Bouma, B.J.M. Mulder, The changing epidemiology of congenital heart disease, Nat. Rev. Cardiol. 8 (1) (2011) 50–60.
[2] N.I. Miyague, S.M. Cardoso, F. Meyer, F.T. Ultramari, F.H. Araújo, I. Rozkowisk, et al., Epidemiological study of congenital heart defects in children and adolescents: analysis of 4,538 cases, Arq. Bras. Cardiol. 80 (3) (2003) 269–278.
[3] Y. Zhou, W.K. Jia, Z. Jian, L. Zhao, C.C. Liu, Y. Wang, et al., Downregulation of microRNA-199a-5p protects cardiomyoblasts in cyanotic congenital heart disease by attenuating endoplasmic reticulum stress, Mol. Med. Rep. 16 (3) (2017) 2992–3000.
[4] J.I.E. Hoffman, Incidence of congenital heart disease: II. Prenatal Incidence J.I.E, Pediatr. Cardiol. 16 (4) (1995) 155–165.
[5] J.I.E. Hoffman, S. Kaplan, The incidence of congenital heart disease, J. Am. Coll. Cardiol. 39 (12) (2002) 1890–1900.
[6] R.N. Ruckman, G.C. Rosenquist, D.A. Rademaker, D.E. Morse, P.R. Getson, The effect of graded hypoxia on the embryonic chick heart, Teratology 32 (3) (1985) 463–472.
[7] M. van den Hoff, Programmed cell death in the developing heart, Cardiovasc. Res. 45 (3) (2000) 603–620.
[8] H.K. Jiang, G.R. Qiu, J. Li-Ling, N. Xin, K.L. Sun, Reduced ACTC1 expression might play a role in the onset of congenital heart disease by inducing cardiomyocyte apoptosis, Circ. J. 74 (2010) 2410–2418.
[9] Y. Zhang, B. Peng, Y. Han, MiR-182 alleviates the development of cyanotic congenital heart disease by suppressing HES1, Eur. J. Pharmacol. 836 (2018) 18–24.
[10] L. Wang, D. Tian, J. Hu, H. Xing, M. Sun, J. Wang, Q. Jian, H. Yang, MiRNA-145 regulates the development of congenital heart disease through targeting FXN, Pediatr. Cardiol. 37 (2016) 629–636.
[11] K.K.A. Sarangapani, C.L. Asbury, Trends Genet, 37 (1) (2012) 62–70. *Trends Genet.*.
[12] H. Carlson, S. Ota, Y. Song, Y. Chen, P.J. Hurlin, Tbx3 impinges on the p53 pathway to suppress apoptosis, facilitate cell transformation and block myogenic differentiation, Oncogene 21 (24) (2002) 3827–3835.
[13] T. Willmer, A. Cooper, J. Peres, R. Omar, S. Prince, The T-Box transcription factor 3 in development and cancer, BioSci. Trends. 11 (3) (2017) 254–266.
[14] C.A. Renard, C. Labalette, C. Armengol, D. Cougot, Y. Wei, S. Cairo, et al., Tbx3 is a downstream target of the Wnt/β-catenin pathway and a critical mediator of β-catenin survival functions in liver cancer, Cancer Res. 67 (3) (2007) 901–910.
[15] Z.F. Miao, X.Y. Liu, H.M. Xu, Z.N. Wang, T.T. Zhao, Y.X. Song, et al., Tbx3 overexpression in human gastric cancer is correlated with advanced tumor stage and nodal status and promotes cancer cell growth and invasion, Virchows Arch. 469 (5) (2016) 505–513.
[16] S. Aliwaini, A. Lubbad, A. Shourfa, H. Hamada, B. Ayesh, H. Abu Tayem, et al., Overexpression of TBX3 transcription factor as a potential diagnostic marker for breast cancer, Mol. Clin. Oncol. 10 (1) (2019) 105–112.
[17] L. Perkhofer, K. Walter, I.G. Costa, M.C.R. Carrasco, T. Eiseler, S. Hafner, et al., Tbx3 fosters pancreatic cancer growth by increased angiogenesis and activin/nodal-dependent induction of stemness, Stem Cell Res. 17 (2) (2016) 367–378.
[18] H. Xie, E. Zhang, N. Hong, Q. Fu, F. Li, S. Chen, et al., Identification of TBX2 and TBX3 variants in patients with conotruncal heart defects by target sequencing, Hum. Genom. 12 (1) (2018) 44.
[19] M.W.M. Knaapen, M.J. Davies, M. De Bie, A.J. Haven, W. Martinet, M.M. Kockx, Apoptotic versus autophagic cell death in heart failure, Cardiovasc. Res. 51 (2) (2001) 304–312.
[20] I.B. Roninson, Oncogenic functions of tumour suppressor p21Waf1/Cip1/Sdi1: association with cell senescence and tumour-promoting activities of stromal fibroblasts, Cancer Lett. 179 (1) (2002) 1–14.
[21] A. Yagi, Y. Hasegawa, H. Xiao, M. Haneda, E. Kojima, A. Nishikimi, et al., GADD34 induces p53 phosphorylation and p21/WAF1 transcription, J. Cell. Biochem. 90 (6) (2003) 1242–1249.
[22] E.W. Lee, M.S. Lee, S. Camus, J. Ghim, M.R. Yang, W. Oh, et al., Differential regulation of p53 and p21 by MKRN1 E3 ligase controls cell cycle arrest and apoptosis, EMBO J. 28 (14) (2009) 2100–2113.
[23] Y. Wang, J.C. Fisher, R. Mathew, L. Ou, S. Otieno, J. Sublet, et al., Intrinsic disorder mediates the diverse regulatory functions of the Cdk inhibitor p21, Nat. Chem. Biol. 7 (4) (2011) 214–221.
[24] H. Zhang, K.J. Menzies, J. Auwerx, The role of mitochondria in stem cell fate and aging, Development 145 (8) (2018) dev143420.
[25] A. Clavier, A. Rincheval-Arnold, J. Colin, B. Mignotte, I. Guénal, Apoptosis in Drosophila: which role for mitochondria? Apoptosis 21 (3) (2016) 239–251.
[26] S. Liang, K. Sun, Y. Wang, S. Dong, C. Wang, L.X. Liu, et al., Role of Cyt-C/caspases-9,3, Bax/Bcl-2 and the FAS death receptor pathway in apoptosis induced by zinc oxide nanoparticles in human aortic endothelial cells and the protective effect by alpha-lipoic acid, Chem. Biol. Interact. 258 (2016) 40–51.
[27] S.C. Ruffolo, D.G. Breckenridge, M. Nguyen, I.S. Goping, A. Gross, S.J. Korsmeyer, et al., BID-dependent and BID-independent pathways for BAX insertion into mitochondria, Cell Death Differ. 7 (11) (2000) 1101–1108.
[28] V.E. Papaioannou, T-box genes in development: from hydra to humans, Int. Rev. Cytol. 207 (2001) 1–70.
[29] S. Wansleben, J. Peres, S. Hare, C.R. Goding, S. Prince, T-box transcription factors in cancer biology, Biochim. Biophys. Acta Rev. Canc. 1846 (2) (2014) 380–391.
[30] E.A. Packham, T-box genes in human disorders, Hum. Mol. Genet. 12 (90001) (2003) 37R–44R.
[31] S. Sundara Rajan, A.M. Hanby, K. Horgan, H.H. Thygesen, V. Speirs, The potential utility of geminin as a predictive biomarker in breast cancer, Breast Canc. Res. Treat. 143 (1) (2014) 91–98.
[32] J. Kajstura, M. Mansukhani, W. Cheng, K. Reiss, S. Krajewski, J.C. Reed, et al., Programmedcell death and expression of the protooncogene bcl-2 in myocytes during postnatal maturation of the heart, Exp. Cell Res. 219 (1) (1995) 110–121.
[33] R.A. Blundell, The biology of p21waf1/cip1 - review paper, Am. J. Biochem. Biotechnol. 2 (1) (2009) 33–40.
[34] J.G. Jackson, V. Pant, Q. Li, L.L. Chang, A. Quintás-Cardama, D. Garza, et al., P53-Mediated senescence impairs the apoptotic response to chemotherapy and clinical outcome in breast cancer, Cancer Cell 21 (6) (2012) 793–806.
[35] P. Witek, A. Korga, F. Burdan, M. Ostrowska, B. Nosowska, M. Iwan, J. Dudka, The effect of a number of H9C2 rat cardiomyocytes passage on repeatability of cytotoxicity study results, Cytotechnology 68 (2016) 2407–2415.